

ORIGINAL RESEARCH

OPEN ACCESS



# CXCL10 and IL15 co-expressing chimeric antigen receptor T cells enhance anti-tumor effects in gastric cancer by increasing cytotoxic effector cell accumulation and survival

Siyue Nie<sup>a,b,c</sup>, Yujie Song<sup>b</sup>, Kun Hu<sup>b</sup>, Wei Zu<sup>d,e</sup>, Fengjiao Zhang<sup>b</sup>, Lixia Chen<sup>b</sup>, Qiang Ma<sup>b</sup>, Zishan Zhou<sup>b</sup>, and Shunchang Jiao<sup>c</sup>

<sup>a</sup>PLA Medical School, Beijing, China; <sup>b</sup>Research and Development Department, Beijing DCTY Biotech Co. LTD, Beijing, China; <sup>c</sup>Department of Oncology, The Fifth Medical Center of Chinese PLA General Hospital, Beijing, China; <sup>d</sup>Department of Functional Neurosurgery, Capital Medical University, Beijing, China; <sup>e</sup>Department of Functional Neurosurgery, Xuanwu Hospital Capital Medical University, Beijing, China

## ABSTRACT

Chimeric antigen receptor (CAR) T cells have demonstrated outstanding therapeutic success in hematological malignancies. Yet, their efficacy against solid tumors remains constrained due to inadequate infiltration of cytotoxic T and CAR-T cells in the tumor microenvironment (TME), a factor correlated with poor prognosis in patients with solid tumors. To overcome this limitation, we engineered CAR-T cells to secrete CXCL10 and IL15 (10 × 15 CAR-T), which sustain T cell viability and enhance their recruitment, thereby amplifying the long-term cytotoxic capacity of CAR-T cells in vitro. In a xenograft model employing NUGC4-T21 cells, mice receiving 10 × 15 CAR-T cells showed superior tumor reduction and extended survival rates compared to those treated with second-generation CAR-T cells. Histopathological evaluations indicated a pronounced increase in cytotoxic T cell accumulation in the TME post 10 × 15 CAR-T cell treatment. Therefore, the synergistic secretion of CXCL10 and IL15 in these CAR-T cells enhances T cell recruitment and adaptability within tumor tissues, improving tumor control. This approach may offer a promising strategy for advancing CAR-T therapies in the treatment of solid tumors.

## ARTICLE HISTORY

Received 2 November 2023  
Revised 2 May 2024  
Accepted 17 May 2024

## KEYWORDS

CAR-T cells; interleukin 15; CXCL10; infiltration; Claudin18.2



## Introduction



Gastric cancer (GC) ranks fifth in global incidence and in fourth mortality among malignant tumors, posing a severe threat to human life.<sup>1</sup> With the advancement and popularity of endoscopic techniques, both the diagnosis and survival rates of early-stage GC have significantly improved.<sup>2</sup> However, treatment for advanced GC is still primarily palliative, including surgery, radiotherapy, chemotherapy, targeted therapy and immunotherapy, with the five-year survival rate remains below 40%. CAR-T cell therapy is being explored as a therapeutic strategy for advanced gastric cancer,<sup>3</sup> showing improved pharmacodynamic effects in animal models with targets including HER2,<sup>4,5</sup> CLDN18.2,<sup>6</sup> and MSLN.<sup>7</sup> Interim results from a phase I clinical trial of CLDN18.2 CAR-T cells (CT041)<sup>8</sup> indicated that the objective response rate (ORR) for 28 patients with gastric cancer and gastroesophageal-junction adenocarcinoma (GC/GEJ) was 57.1%, and the six-month overall survival rate was 81.2%. While these findings are supportive of CAR-T cell therapy's potential in solid tumors, its comparative efficacy remains lower than that observed in hematological malignancies, where the complete response (CR) rate can reach up to 90%. Research identifies T-cell infiltration within the tumor microenvironment (TME) of solid tumors as an important factor influencing the efficacy of CAR-T cell therapy, partly because


the tumor microenvironment (TME) presents challenges such as a dense extracellular matrix, inappropriate migration signals, and various immunosuppressive mechanisms.<sup>9–11</sup> These factors impede the effective accumulation and survival of T-cells,<sup>12</sup> including CAR-T cells, and are associated with a poorer prognosis. Consequently, transforming the TME to support T-cell infiltration and persistence is a critical objective.<sup>13</sup>

The chemokine network is essential for regulating immune cell circulation, homing, recruitment, and retention. Chemokine receptors are predominantly expressed on immune cells, enable these cells to navigate toward concentration gradients of corresponding chemokines.<sup>14</sup> However, most TME often exhibit chemokine secretion patterns that promote pro-tumor immune cell recruitment and suppress anti-tumor responses by modulating chemokine levels and types.<sup>15</sup> Notably, chemokines that recruit primarily anti-tumor immune cells are usually found at low levels, leading to weak recruitment signals. This results in insufficient infiltration and ineffective immune responses from cytotoxic T cells, which promotes immune escape and tumor growth. Therefore, enhancing the concentration of specific chemokines in TME is a critical strategy for increasing the accumulation of anti-tumor effector cells.

CXCL10, a critical chemokine located on human chromosome 4 (q12–21), is secreted by monocytes and some

**CONTACT** Shunchang Jiao  [jiaosc@vip.sina.com](mailto:jiaosc@vip.sina.com)  Department of Oncology, The Fifth Medical Center of Chinese PLA General Hospital, No.28 Fuxing Road, Beijing 100853, China; Zishan Zhou

 [zsz@taiyuanshengwu.com](mailto:zsz@taiyuanshengwu.com)  Beijing DCTY Biotech Co. LTD, No.86 Shuangying West Road, Beijing 102200, China

 Supplemental data for this article can be accessed online at <https://doi.org/10.1080/2162402X.2024.2358590>

© 2024 The Author(s). Published with license by Taylor & Francis Group, LLC.

This is an Open Access article distributed under the terms of the Creative Commons Attribution-NonCommercial License (<http://creativecommons.org/licenses/by-nc/4.0/>), which permits unrestricted non-commercial use, distribution, and reproduction in any medium, provided the original work is properly cited. The terms on which this article has been published allow the posting of the Accepted Manuscript in a repository by the author(s) or with their consent.

tumor cells within the TME. This chemokine attracts circulating CXCR3+ T cells and NK cells to tumor sites, enhancing the anti-tumor immune response.<sup>16</sup> Higher levels of CXCL10 in tumors are associated with better prognoses in non-small cell lung cancer<sup>17,18</sup> and rectal cancer.<sup>19</sup> Consequently, increasing CXCL10 secretion in the TME may be a pivotal strategy to potentially boost the recruitment of CXCR3+ immune cells (T and NK cells). Studies have demonstrated that methods such as induced tumor cell secretion,<sup>20</sup> fusion proteins,<sup>21</sup> and small-molecule ROR $\gamma$ t agonists<sup>22</sup> can effectively elevate CXCL10 levels, thereby enhancing recruitment signals and promoting the aggregation of immune cells. Additionally, chemokine-modified CAR-T cells have been employed to strengthen recruitment signals in the TME, leading to increased T cell infiltration. However, research into CAR-T cell modifications involving CXCL10 remains relatively rare.

Interleukin-15 (IL-15) is a cytokine in  $\gamma$ c family and is located on human chromosome 4q31. The IL-15 receptor comprises three subunits:  $\alpha$ ,  $\beta$ , and  $\gamma$ c.  $\beta$  and  $\gamma$ c subunits are also components of the IL-2 receptor and are expressed in T cells. IL-15 interaction with its receptor activates kinase classes – JAK, Shc, and PI3K – and their downstream pathways, supporting T cell proliferation and survival. Compared to IL-2, CAR-T cells cultured with IL-15 retain a less differentiated stem cell memory (TSCM) phenotype.<sup>23</sup> Additionally, IL-15 has been employed to arm VEGFR2 CAR-T cells, improving their anti-apoptotic properties and tumor suppression in B16 melanoma models.<sup>24</sup> IL15-modified GD2 CAR-T cells have demonstrated effective tumor control in glioblastoma xenograft model.<sup>25</sup>

Recent studies have explored enhancing CAR-T cells with interleukins and chemokines, which have demonstrated an improved anti-tumor effect. A study by Adachi et al. showed that  $7 \times 10^9$  CAR-T cells, co-expressing IL-7 and CCL19, not only increased the infiltration of dendritic cells and T cells but also notably extended survival rates.<sup>26</sup> In a Phase I clinical trial,<sup>27</sup> this treatment led to complete remission in one pancreatic cancer patient (1/6, 16.7%) and partial remission in one hepatocellular carcinoma patient (1/6, 16.7%), with two other patients (2/6, 33.3%) achieving stable disease, indicating the potential of these cells in treating advanced solid tumors. Furthermore, CAR-T cells enhanced with IL-7 and CCL21 have been shown to increase efficacy and sustain T-cell persistence in mouse tumor models, supporting the benefits of interleukin and chemokine co-modification.<sup>28</sup> IL-15-CCL19 NKG2D-CAR-T cells were also effective in expanding T-cell populations and enhancing anti-tumor responses in a zebrafish tumor model.<sup>29</sup> To date, CAR-T cells co-modified with CXCL10 and IL-15 have not yet been reported.

Here we selected CLDN18.2, a key antigenic target in gastric tumors, to construct CAR-T cells that secrete both CXCL10 and IL15 (10  $\times$  15 CAR), and assessed their effects both in vitro and in vivo. CXCL10 and IL15 secretion from these CAR-T cells promoted antitumor activity by enhancing cytotoxic T cell accumulation and viability at the tumor site.

## Materials and methods

### Mice and cell lines

Female NOG mice (6–8 weeks old) were purchased from Charles River (Beijing, China), and male NCG mice (6–8 weeks old) were purchased from Gempharmatech (Jiangsu, China). 293T cells were obtained from ATCC. NUGC4-T21 monoclonal cells stably expressing CLDN18.2, GFP, and Luciferase were established and maintained in our laboratory. 293T and NUGC4-T21 cells were respectively grown in DMEM (Gibco) or RPMI-1640 (Gibco) with 10% FBS (Gibco).

### Vectors and constructs

A two-generation anti-CLDN18.2 CAR construct (28z CAR) comprises a CD8 signal peptide, an anti-CLDN18.2 single-chain fragment variable (scFv), a CD8 transmembrane region, a CD28 co-stimulatory domain, and a CD3 $\zeta$  intracellular activation region. To construct CAR-T cells that secrete CXCL10 and IL15, human CXCL10 and IL15 sequences synthesized by Genewiz (Suzhou, China) were linked by T2A after 28z CAR. The lentiviral vector pCDH was the backbone for all CAR constructs.

### In vivo anti-tumor models

Animal experiments were reviewed and approved by the Institutional Animal Care and Use Committee (IACUC) at Yicon Beijing Biomedical Technology Inc. (YK-IACUC-2023-006) and Beijing Vitalstar Biotechnology Co. (VST-SY-20230712). The NOG and NCG mice were subcutaneously incubated with  $5 \times 10^6$  NUGC-T21 cells in 100  $\mu$ l PBS in the right flank. Twelve days later, CAR-T cells in 200  $\mu$ l PBS were intravenously via the tail vein. Tumor volumes were measured with Vernier calipers and calculated according to the formula: Tumor volume = length  $\times$  width<sup>2</sup>  $\times$  0.5.

### Statistical analysis

GraphPad Prism 9.5 software was used for statistical analysis. An unpaired two-tailed Student's t-test was used to analyze the differences between two groups. For comparisons between more than two groups, one-way ANOVA and two-way ANOVA were performed to compare statistical differences. The Kruskal-Wallis test compares data across three or more non-normally distributed groups. Log-rank test was applied to assess survival curves. All experiments were conducted in at least duplicate. The statistical differences are presented in the figures (\* $p < 0.05$ , \*\* $p < .01$ , \*\*\* $p < .001$ , \*\*\*\* $p < .0001$ ).

## Results

### Building a CLDN18.2 CAR-T cell secreting IL15 and CXCL10

We constructed 10, 15, and 10  $\times$  15 CAR-T cells to assess the multiple effects of CXCL10 and IL15 (Figure 1a). CXCL10 and IL15 were linked via a T2A peptide following the CLDN18.2 CAR structure, creating human-derived 10/15/10  $\times$  15 CAR structures (Figure 1b).

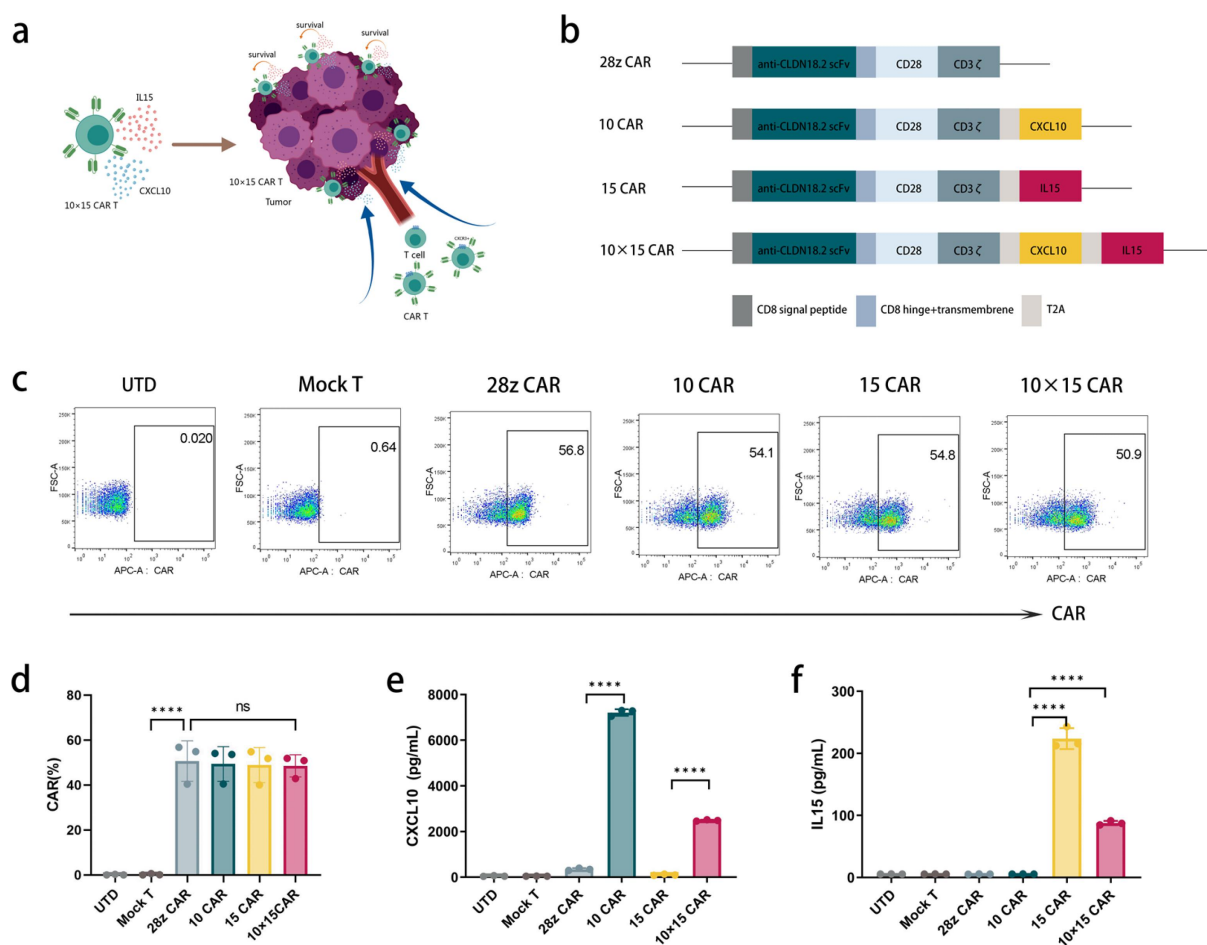


**Figure 1.** 10 × 15 CAR-T construction. (a) Schematic representation of 10 × 15 CAR-T antitumor function. (b) Constructs of 28z CAR and cytokine expressing-CARs. (c) Representative flow cytometry data of CAR expression after 5 days transduction. (d) CAR-T cells ratios in T cells after 5 days of transduction (n = 3). (e) and (f) 1 × 10<sup>6</sup> CAR-T cells were incubated for 24 h and then ELISA was performed to detect the secretion of CXCL10 and IL15 (n = 3). Each experiment was repeated at least three times independently, results are exhibited as mean ± SD. Statistical analysis was performed using one-way ANOVA. UTD means untransduced T cells. Mock T indicates transfected lentivirus vector. \*\*\*\*p < .0001.

Lentiviruses carrying these CAR constructs, produced in 293T cells, were used to transduce activated human T cells. Five days after transduction, we evaluated cell surface CAR expression using flow cytometry and found no significant differences in the expression of the 10 × 15 CAR compared to the other groups (Figure 1c,d). Additionally, the secretion of CXCL10 and IL15 by the 10 × 15 CAR-T cells was significantly higher than that by the 28z CAR cells (Figures 1e,f), confirming the successful creation of 10 × 15 CAR-T cells that simultaneously express CAR, CXCL10, and IL15.

### IL15 and CXCL10 provided long-lasting cytotoxic effect to CAR-T cells

To evaluate the possible impacts of CXCL10 and IL15 on the malignant behaviors of NUGC4-T21 and 293T cells, we first measured the expression of CXCR3 (the CXCL10 receptor) and IL-15 Rβ and γ subunits (components of the IL15 receptor) in these cells. Neither CXCR3 nor the IL15β and γ subunits showed significant expression on either cell type (Figure S3). Furthermore, we explored the influence of CXCL10 and IL15 on the epithelial-mesenchymal transition (EMT) phenotype by measuring E-cadherin and N-cadherin expression in

both cell lines (Figure S4). N-cadherin levels remained low and unchanged under the treatment conditions. Conversely, E-cadherin levels were higher in the absence of CXCL10 and IL15, with 293T cells showing 98.4% and NUGC4-T21 cells 80.9% expression. There was no significant reduction after exposure to 10 ng/ml of either cytokine (Figure S4b and d). Additionally, we assessed the effect of various concentrations of CXCL10 and IL15 on cell proliferation and observed no notable changes across different cytokine doses (10 ng/ml, 5 ng/ml, 2.5 ng/ml, 1.25 ng/ml, and 0 ng/ml) in both cell types (Figure S5). These results indicate that CXCL10 and IL15 did not significantly influence the proliferation or EMT phenotype of NUGC4-T21 and 293T cells, providing a foundation for further comparative studies involving various CAR-T cells co-cultured with target cells or used in vivo anti-tumor assays.

Four groups of CAR-T cells were co-cultured with NUGC4-T21 cells at effector-to-target (E/T) ratios of 5:1, 2.5:1, and 1.25:1. Nine hours post-incubation, no significant differences were observed in the cytotoxic efficacy of the CAR-T cells at these respective E/T ratios (Figure 2a). Additionally, CAR-T cells were co-cultured with NUGC4-T21 cells at a 1:1 E/T ratio, and IFN-γ and CD107a expressions were assessed. The expression levels of IFN-γ and

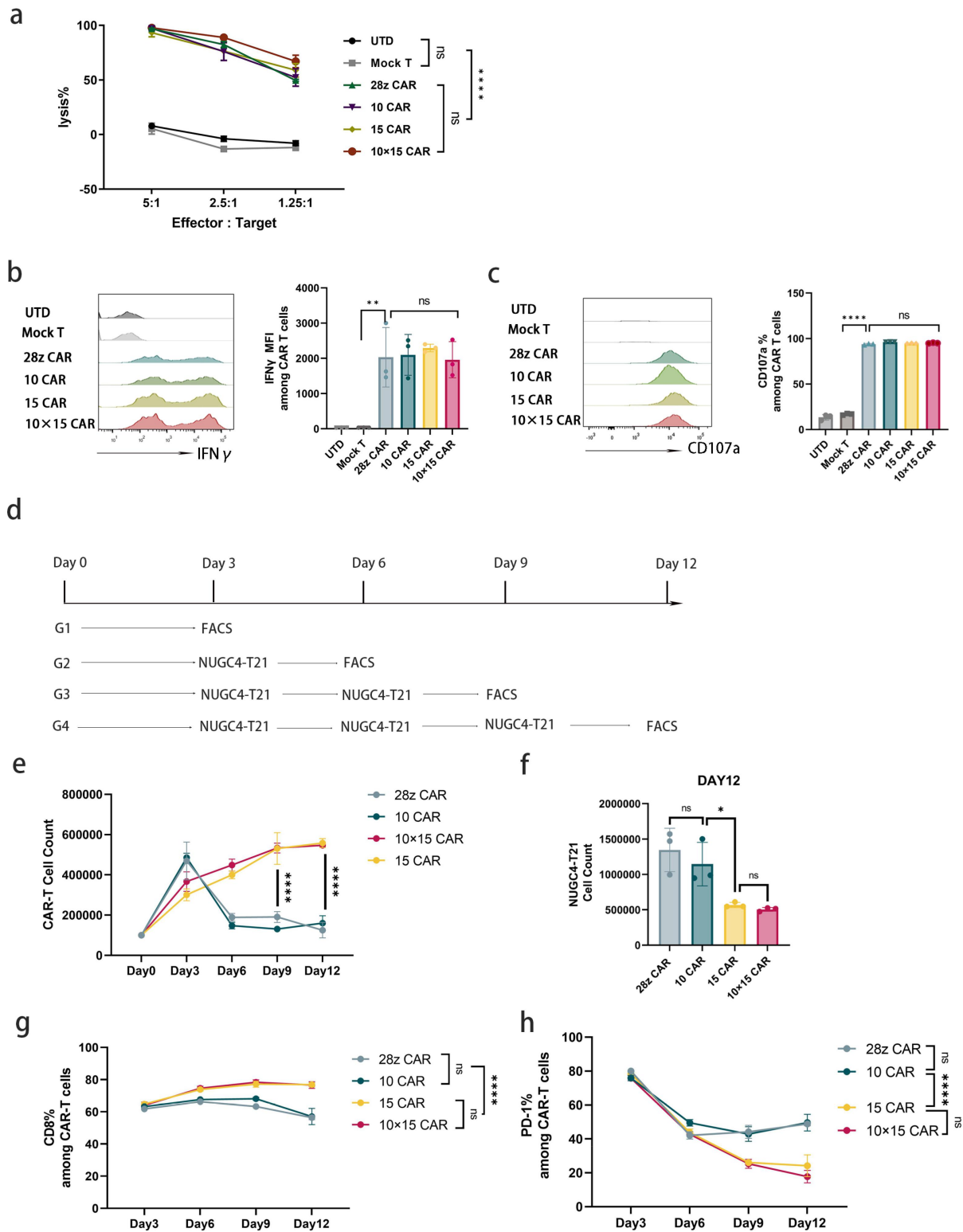


**Figure 2.** In vitro cytotoxicity function of  $10 \times 15$  CAR-T cells. (a) Luciferase-expressing NUGC4-T21 cells were incubated with CAR-T cells at three effector-to-target (E/T) ratios for 9 h. The cytotoxicity was evaluated using a luciferase-based assay ( $n = 3$ ). Following stimulation at a 1:1 E/T ratio for 24 hours, IFN- $\gamma$  mean fluorescence intensity (MFI) (b) and the percentage of CD107a+ CAR-T cells (c) were quantified using flow cytometry ( $n = 3$ ). (d) Overview of the rechallenge experiment: CAR-T cells and NUGC4-T21 cells were co-cultured at a 1:5 E/T ratio on Day 0 across four groups. An additional  $5 \times 10^5$  NUGC4-T21 cells were added on Day 3 (Groups 2, 3 and 4), Day 6 (Group 3 and 4), and Day 9 (Group 4) per well. Absolute cell counts for both CAR-T and NUGC4-T21 cells were determined using flow cytometry (e)-(f) ( $n = 3$ ). The proportions of CD8+ and PD-1+ CAR-T cells were also analyzed (g)-(h) ( $n = 5$ ). Each experiment was conducted independently at least three times. Data are presented as mean  $\pm$  SD (a, b, c, e, and f) or mean  $\pm$  SEM (g and h). Statistical analysis was performed using one-way ANOVA (b, c, and f) and two-way ANOVA (a, e, g, and h). \* $p < .05$ , \*\* $p < .01$ , \*\*\*\* $p < .0001$ .

CD107a were not significantly different among the four groups (Figure 2b,c). This indicated that the cytokines IL15 and CXCL10, secreted by CAR-T cells, did not significantly influence the cytotoxic function of CAR-T cells on NUGC4-T21 during the brief co-incubation period.

To assess recursive killing, we established four experimental groups (G1, G2, G3, and G4), each containing four subgroups involving the CAR-T cell types 28z, 10, 15, and  $10 \times 15$ . Initially, each subgroup co-cultured  $1 \times 10^5$  CAR-T cells with  $5 \times 10^5$  NUGC-T21 cells on Day 0. Additional NUGC-T21 cells ( $5 \times 10^5$  per well) were added to G2 on Day 3, to G3 on Days 3 and 6, and to G4 on Days 3, 6, and 9. Absolute CAR-T cell counts for G1, G2, G3, and G4 were measured on Days 3, 6, 9, and 12, respectively, as shown in Figure 2d; the flow cytometry strategy is detailed in Figure S2. By Day 9, the counts for the 15 and  $10 \times 15$  CAR-T cells surpassed those of the 28z and 10 CAR-T cells, as shown in Figure 2e. On Day 12, the groups with 15 and  $10 \times 15$  CAR-T cells exhibited significantly fewer remaining live NUGC-T21 cells compared to the 28z and 10 CAR groups, as detailed in Figure 2f.

The phenotypes of CD8+ and PD-1+ CAR-T cells were analyzed with the flow cytometry strategy shown in Figure S1. Results demonstrated a gradual increase in the proportion of CD8+ cells in the 15 and  $10 \times 15$  CAR-T cell groups from Day 3 to Day 12, whereas changes in the 28z and 10 CAR groups were minimal. As a result, the percentage of CD8+ CAR-T cells was significantly higher in the 15 and  $10 \times 15$  CAR groups than in the 28z and 10 CAR groups (Figure 2g). Additionally, the initial percentage of PD-1+ CAR-T cells was high in all groups on Day 3. Importantly, the proportion of PD-1+ CAR-T cells was significantly lower in the IL15-secreting CAR-T groups (15 CAR and  $10 \times 15$  CAR) compared to the 28z and 10 CAR groups during repeated challenges with NUGC4-T21 cells (Figure 2h). Moreover, no notable statistical difference was observed between the 28z and 10 CAR groups. These findings suggest that IL15 secretion might decrease the proportion of PD-1+ CAR-T cells, while CXCL10 secretion does not significantly affect this proportion. Therefore, the results of this section suggested that in short-term co-cultures with NUGC4-T21, the secretion of IL15 and CXCL10 did not significantly influence the cytotoxic activity of CAR-T cells. Interestingly, in prolonged co-cultures, IL15-modified CAR-T cells (15 CAR and  $10 \times 15$  CAR) were more numerous than that of the 28z CAR and 10 CAR, exhibiting a higher proportion of CD8+ cells and a lower proportion of PD-1+ exhausted cells. This is consistent with results of most studies<sup>23–24</sup> that IL15 secretion may have been primarily responsible for promoting the proliferation of CAR-T cells. This cytokine secretion was also instrumental in the expansion of CD8+ CAR-T cells and in reducing the proportion of exhausted CAR-T cells.

### **IL15 improved $10 \times 15$ CAR-T cell expansion, survival, and fitness**

Given that many studies have demonstrated that IL15 modification enhances CAR-T cell expansion, we analyzed the proliferation, amplification, and viability of  $10 \times 15$  CAR-T cells in an IL-free medium. By day 4, the numbers of 15 CAR and  $10 \times 15$  CAR-T cells were marginally higher. By day 6, the

proliferation rates of these groups significantly exceeded those of their non-IL15-modified counterparts, the 28z CAR and 10 CAR-T cells (Figure 3a,b). Moreover, cell viability under IL-free conditions showed marked differences; the viability of 28z CAR and 10 CAR-T cells did not exceed 50% by day 4 and declined further by day 6. In contrast, 15 CAR and  $10 \times 15$  CAR-T cells consistently maintained high survival rates (Figure 3c). Additionally, we examined the degree of cell division in  $10 \times 15$  CAR-T cells and observed that, similar to 15 CAR-T cells, they divided more than the 28z CAR and 10 CAR cells under interleukin-free culture conditions (Figure 3d). This suggests that  $10 \times 15$  CAR-T cells can effectively promote cell proliferation and maintain viability even in the absence of exogenous interleukin-15.

We further analyzed the essential phenotypes of  $10 \times 15$  CAR-T cells. After culturing CAR-T cells in an IL-free medium for two days, the proportion of CD8+ T cells was significantly higher in the 15 CAR and  $10 \times 15$  CAR groups than in the remaining two groups (Figure 3e). Given the role of IL15 in the maintenance of T-cell stemness phenotype,<sup>30</sup> we analyzed the TSCM phenotype across four CAR-T cell groups. Our findings indicated that the proportion of TSCM phenotype was substantially elevated in the CAR-T groups secreting IL15 compared to the other two groups (Figure 3f). This suggests that IL15 secretion by  $10 \times 15$  CAR-T cells is crucial for maintaining memory stem cells and enhancing their differentiation potential.

### ***10 × 15 CAR-T cells promoted long-term T-cell recruitment***

To evaluate CAR-T cells recruitment, we initially assessed the expression of CXCR3, a receptor for CXCL10, in T cells. CXCR3 expression in naïve T cells was only 27.4% but increased to 95% after six days of activation (Figure 4a,b). CXCR3 expression remained high in four CAR-T cell groups without significant differences (Figure 4c,d). In both the 10 CAR and  $10 \times 15$  CAR-T cell groups, CXCR3 expression was not significantly down-regulated, indicating that CXCL10-secreting CAR-T cells might possess recruitment capabilities for both T cells and other CAR-T cells. Subsequently, we confirmed the effect of CXCL10 on T-cell migration using transwell assays (Figure 4e). T-cell migration rates increased with higher concentrations of CXCL10 (Figure 4f), which was consistent with many studies.

We assessed CXCL10 concentrations in supernatants from four CAR-T cell groups after culturing in IL-free medium for three days. CXCL10 levels were measured using ELISA (Figure 4g). The 10 CAR and  $10 \times 15$  CAR groups showed significantly higher CXCL10 concentrations compared to the CXCL10-unmodified groups (28z CAR and 15 CAR-T cells). Notably, the  $10 \times 15$  CAR group had elevated CXCL10 secretion levels relative to the 10 CAR group during IL-free incubation, potentially due to IL15 enhancing proliferation. Additionally, T-cell recruitment was evaluated using a transwell assay with these supernatants (Figure 4h). We found that migration rates correlated with CXCL10 concentrations. Enhanced T-cell recruitment was observed in the CXCL10-modified groups, particularly the  $10 \times 15$  CAR group, which demonstrated superior T-cell recruitment compared to the 10 CAR group.

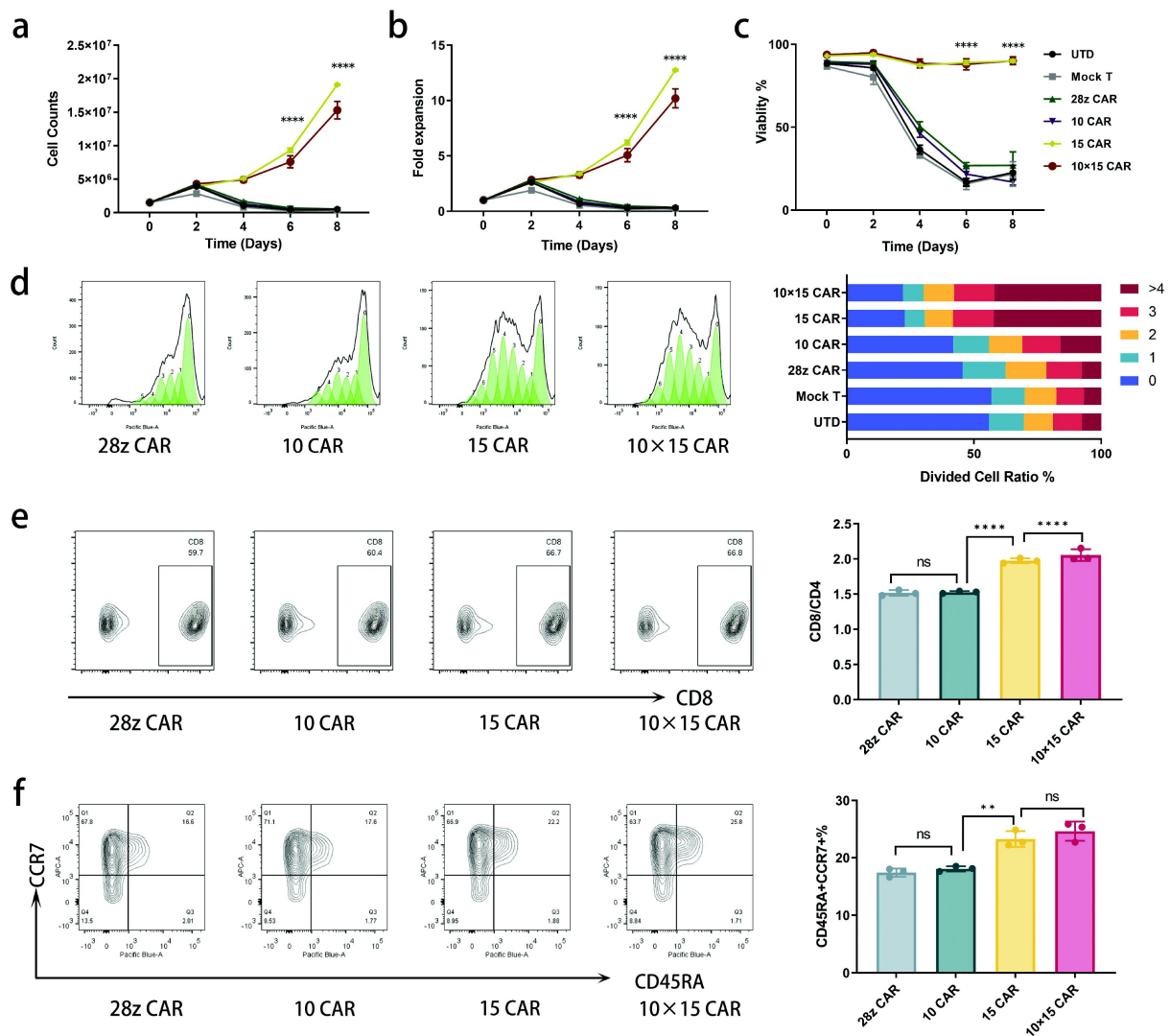


**Figure 3.** IL15 enhances the expansion, viability, and stemness of CAR-T cells. Expansion number (a), expansion fold (b), and cell viability (c) of CAR-T groups at different culture times without additional ILs ( $n = 3$ ). (d) Different CAR-T cells cultured in ILs-free medium were measured by CellTrace Violet at day 4. The numbers 0 to 6 indicate increasing degrees of cell division, with higher numbers reflecting more extensive cell division. The graph depicts the percentage of cells at each degree of division, represented as follows: no division (0, blue), minimal division (1, green), moderate division (2, orange), substantial division (3, red), and extensive division (>4, dark red). (e) CD8 ratios in CAR-T cells cultured without additional ILs ( $n = 3$ ). (f) The TSCM ratio in CAR-T cells was determined by CD45RA and CCR7 expression ( $n = 3$ ). Each experiment is performed at least three times with independent replicates. Results are shown as mean  $\pm$  SD. Statistical analysis was performed using one-way ANOVA (e and f) and two-way ANOVA (a, b, and c). \*\* $p < .01$ , \*\*\*\* $p < .0001$ .

We also collected supernatants from co-cultures of NUGC4-T21 and CAR-T cells after 72 hours and analyzed their effects on T-cell migration (Figure 4i). The CXCL10-modified groups recruited significantly more T cells than the non-CXCL10 modified groups. Interestingly, no significant difference in T-cell migration rates between the 10 CAR and 10  $\times$  15 CAR groups. After seven days of co-culture, we assessed long-term recruitment effects from collected supernatants (Figure 4j). The 10  $\times$  15 CAR group showed significantly greater T-cell recruitment than the 10 CAR group, likely due to IL15 secreted by the 10  $\times$  15 CAR-T cells promoting both CAR-T cell proliferation and CXCL10 secretion, resulting in a stronger recruitment effect.

### 10 $\times$ 15 CAR-T cells demonstrated better anti-tumor effects

We established NUGC4-CLDN18.2 xenograft models to evaluate the antitumor efficacy of 10  $\times$  15 CAR-T cells. NOG mice

were subcutaneously injected with  $5 \times 10^6$  NUGC4-T21 cells on day 0 and treated with  $1 \times 10^6$  CAR-T cells of varying types on day 12. T cell infiltration in tumor and normal tissues was assessed on day 30 (Figure 5a). We compared tumor growth volumes from day 12 to day 30 across different treatment groups and found that all four CAR-T cell groups demonstrated higher tumor suppression rates than those treated with PBS and Mock T cells (Figure 5b,c). Notably, the 10 CAR group exhibited marked tumor inhibition compared to the 28z CAR group, though both groups experienced progressive tumor growth. Furthermore, tumors treated with IL15-secreting CAR-T cells demonstrated more significant regression compared to those in the other two groups. Moreover, the regression was notably more pronounced in the 10  $\times$  15 group than in the 15 group.

IL-15 levels in peripheral blood were measured on days 13, 21, and 28 using ELISA (Figure 5d). By day 13, IL-15 concentrations were notably elevated in the 15 CAR and 10  $\times$  15 CAR

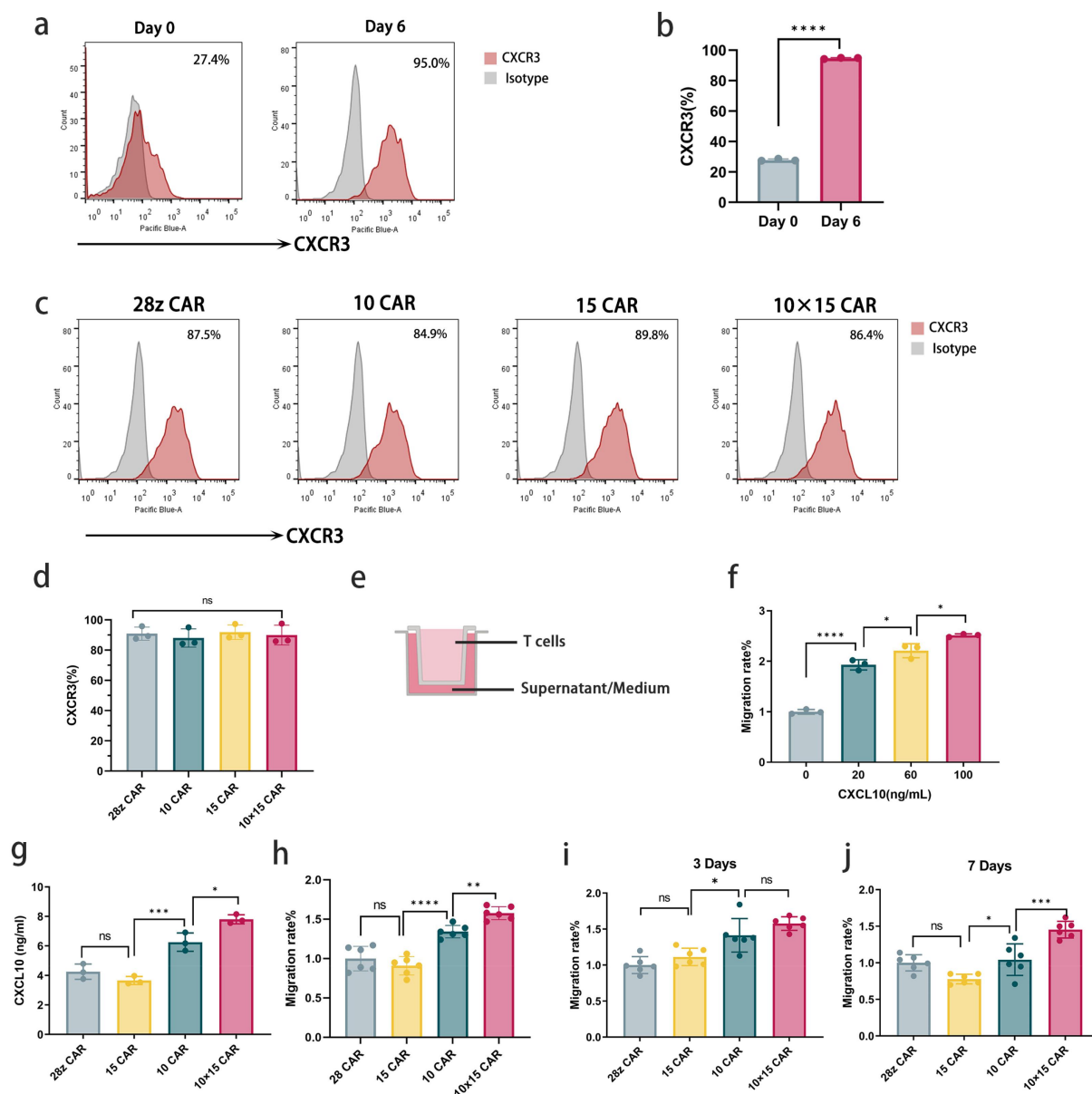


**Figure 4.**  $10 \times 15$  CAR-T cells promoted long-term T-cell recruitment. (a)-(b) Comparison of CXCR3 expression in T cells at inactivation (Day 0) versus activation state after 6 days (Day 6) ( $n = 3$ ). (c)-(d) CXCR3 expression in four groups of CAR-T cells following a 6-day activation ( $n = 3$ ). (e) Schematic diagram of Transwell assay. CXCL10 recombinant protein or CAR-T supernatant in the lower chamber and activated T cells ( $2 \times 10^5$ ) in the upper chamber. Cells in the lower chamber were counted after incubation. (f) Activated CD3+ T cells in the upper chamber were exposed to varying concentrations of CXCL10 recombinant protein in the lower chamber for 5 hours. Cells migrated to the lower chamber were quantified, using 0 ng/mL as the control to calculate the migration index ( $n = 3$ ). (g) and (h). CAR-T cells ( $1 \times 10^6$ ) cultured for 3 days, and CXCL10 concentration in supernatants (g) were measured ( $n = 3$ ). T cell migration rates from these supernatants (h) were tested ( $n = 6$ ). (i)-(j). CAR-T cells ( $1 \times 10^5$ ) co-cultured with NUGC4-T21 for 3 days (E: T = 1:3) (i) and 7 days (E: T = 1:5) (j). T cell migration rates of these supernatants were assayed ( $n = 6$ ). 28z CAR group served as the control for migration rate calculations. Experiments were conducted at least three times with consistent results. Data are presented as mean  $\pm$  SD. Statistical analysis was performed using unpaired two-tailed Student's t-test (b) or one-way ANOVA (d, f, g, h, i, and j). \* $p < .05$ , \*\* $p < .01$ , \*\*\* $p < .001$ , \*\*\*\* $p < .0001$ .

groups compared to the other two groups, verifying successful in vivo secretion of IL-15. This secretion increased substantially by day 28, with IL-15-modified CAR-T cells sustaining appreciably higher levels than the non-IL15-modified groups, and the 15 CAR group surpassing the  $10 \times 15$  CAR group. Additionally, these enhanced levels were likely correlated with increased proportions of CD3+ T cells and CAR-T cells in peripheral blood (Figure 5f,g). No substantial differences were observed among the four groups on days 13 and 21; however, the proportion of T cells on day 21 was markedly lower than on day 13. By day 28, the proportions of CD3 and CAR-T cells in the 15 CAR and  $10 \times 15$  CAR groups were considerably higher than those in the

28z CAR and 10 CAR groups. The IL-15 modified groups also exhibited a noticeable increase in CAR-T cell proportions on day 28 compared to day 21, likely owing to the IL-15's role in promoting CAR-T cell proliferation.

Additionally, we analyzed serum levels of CXCL10 (Figure 5e). On day 13, the CXCL10-modified CAR-T cells demonstrated elevated serum concentrations compared to the other groups, with the 10 CAR group displaying a slight but not statistically meaningful trend toward higher levels than the  $10 \times 15$  CAR group. From day 21 onward, the CXCL10 levels in the  $10 \times 15$  CAR group surpassed those in the 10 CAR group, likely because IL-15 within the  $10 \times 15$  CAR group

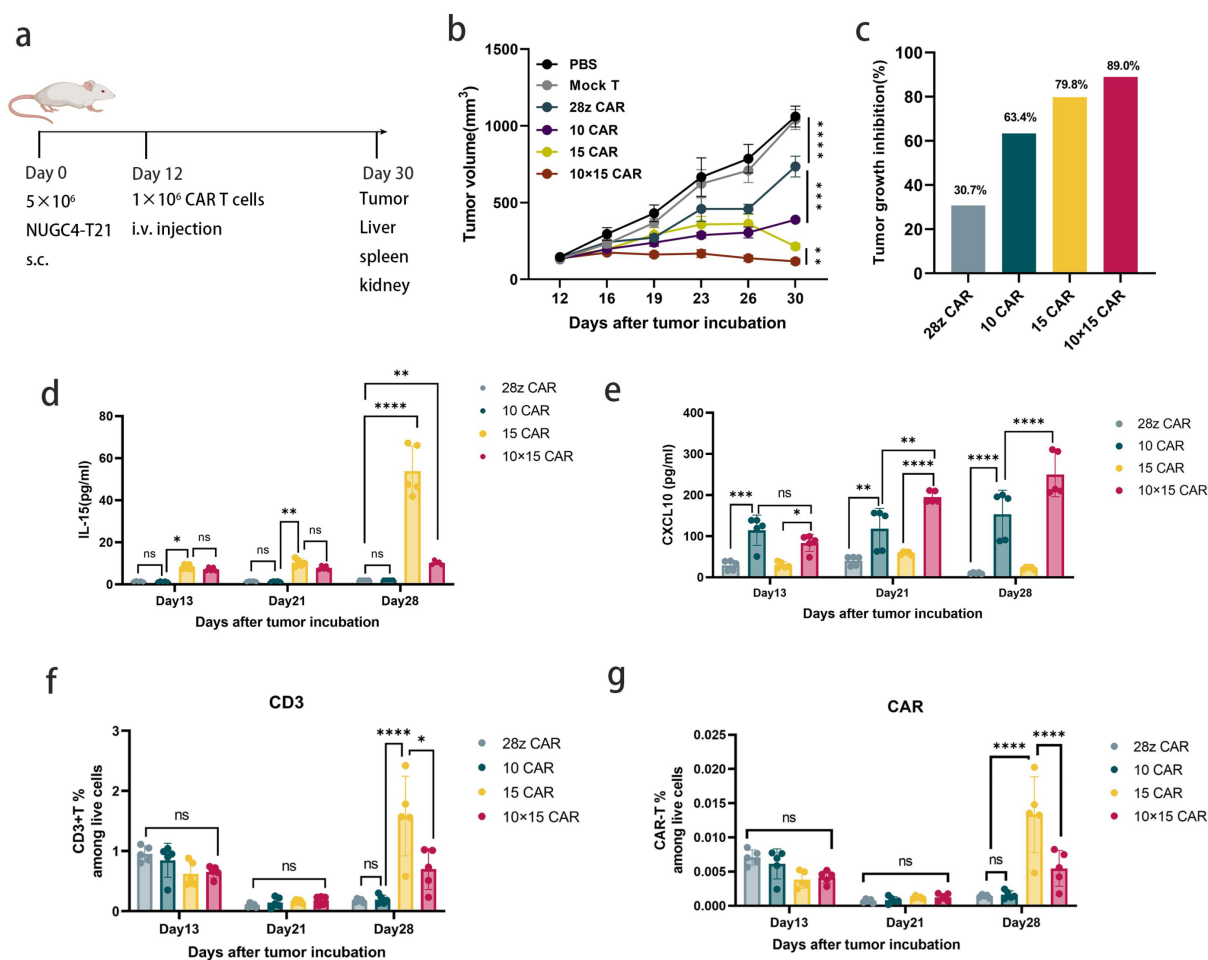


**Figure 5.** Enhanced Anti-Tumor Efficacy of  $10 \times 15$  CAR-T cells in an NUGC4-T21 xenograft model. (a) Experimental setup for the in vivo anti-tumor assay: NOG mice were subcutaneously injected with  $5 \times 10^6$  NUGC4-T21 cells, followed by an intravenous injection of  $1 \times 10^6$  CAR-T cells into the tail vein on day 12. The experiment concluded on day 30, with tumor tissues preserved for paraffin embedding and liver, spleen, and kidney samples analyzed by flow cytometry (FACS) ( $n = 5$  mice per group). (b) Tumor volumes were measured biweekly using vernier calipers. (c) The tumor growth inhibition rates for four CAR-T cell groups on day 30 were calculated, using the PBS group as a control. (d)-(e) Serum concentrations of IL15 (d) and CXCL10 (e) were measured using ELISA on days 13, 21, and 28. (f)-(g) The Frequencies of CD3+ T cells (f) and CAR-T cells (g) in peripheral blood were analyzed by flow cytometry on days 13, 21, and 28. Each experiment was replicated at least three times. Results are presented as mean  $\pm$  SD (d, e, f, and g) or mean  $\pm$  SEM (b). Data were analyzed statistically through two-way ANOVA. \* $p < .05$ , \*\* $p < .01$ , \*\*\* $p < .001$ , \*\*\*\* $p < .0001$ .

supported the viability of CAR-T cells and promoted their CXCL10 secretion. These results indicated the three components of  $10 \times 15$  CAR-T cells – CAR, CXCL10, and IL-15—were successfully expressed in vivo and demonstrated significant tumor regression in the NUGC4-CLDN18.2 xenograft models.

#### ***10 x 15 CAR-T cells increased T-cell accumulation within tumors and extended survival times in vivo***

To evaluate T-cell infiltration, we conducted immunohistochemical analysis using CD3 antibodies on tumors extracted from mice on day 30. Results showed that the  $10 \times 15$  CAR group exhibited significantly higher levels of T-cell accumulation compared to the three groups (Figure 6a,b). Additionally, this group displayed a marked increase in CD8+ T cells and CD8+ Granzyme B+ T cells relative to their counterparts (Figure 6c-e). These findings suggest that the augmented recruitment of cytotoxic T cells,

mediated by CXCL10 and IL15, likely enhances tumor suppression with the  $10 \times 15$  CAR-T treatment.

Further flow cytometry analysis of normal tissues (liver, kidney, and spleen) revealed no notable differences in CD3+ and CD8+ T cell proportions between the  $10 \times 15$  CAR and the 28z CAR groups, although the former showed slightly elevated levels in spleen. Conversely, the 15 CAR group showed significantly higher infiltration levels of CD3+ T cells in the spleen and kidney compared to the second-generation CAR groups, as well as elevated levels of CD8+ T cells in the liver, spleen, and kidney (Figure S6). This indicates that T cell proliferation in liver, kidney, and spleen with the  $10 \times 15$  CAR treatment is comparable to that with second-generation CAR-T cells. Survival time assessments of mice treated with 15 CAR and  $10 \times 15$  CAR (Figure 6f) indicated that the latter group experienced significantly longer survival times (Figure 6g) and more stable body weights (Figure 6h). These results confirm that the  $10 \times 15$  CAR-T treatment offers enhanced anti-tumor effects and improved survival.



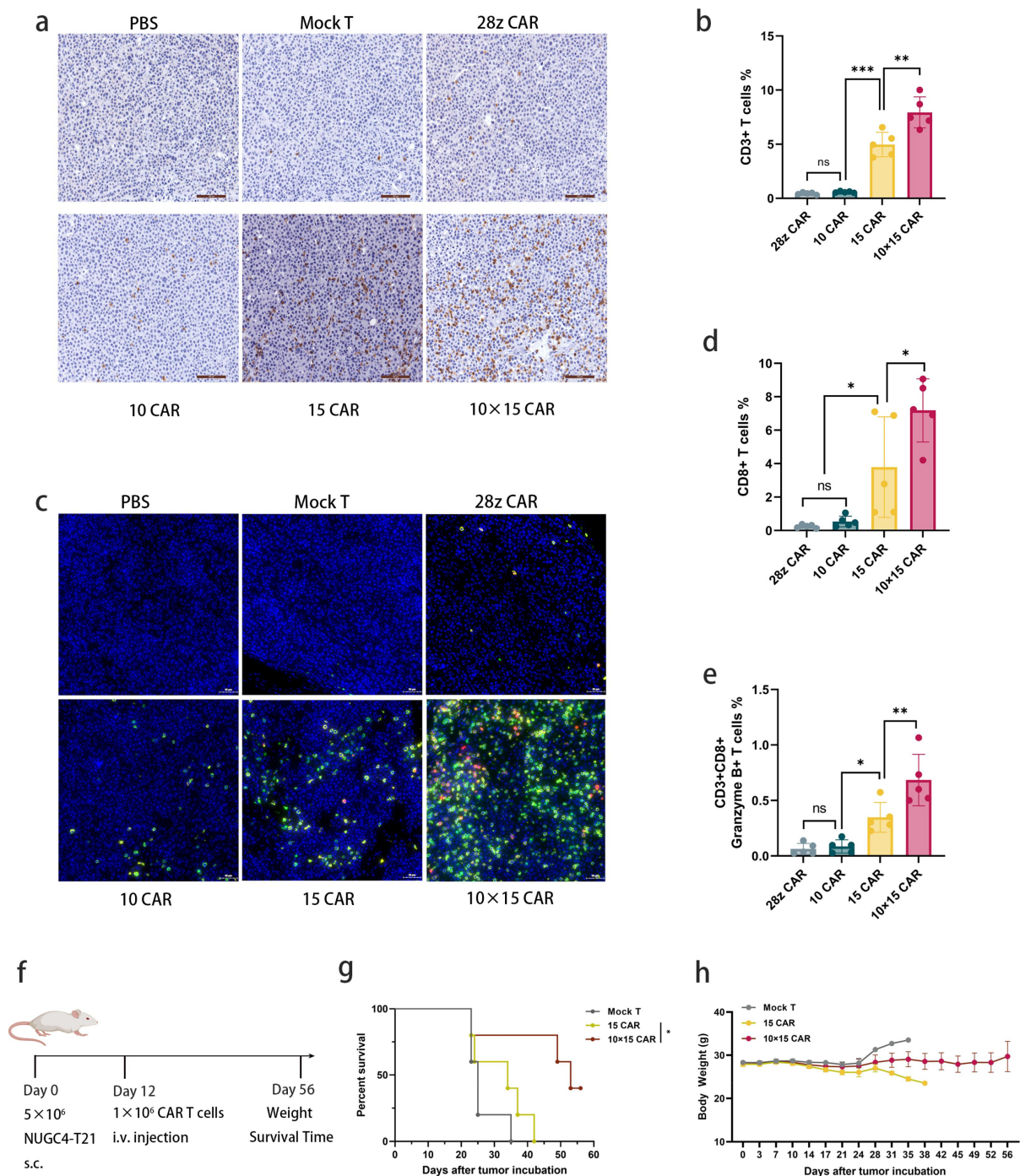


**Figure 6.** Treatment with  $10 \times 15$  CAR-T cells increased T-cell infiltration within tumors and extended survival times in the NUGC4-T21 Xenograft model. Twelve days post-inoculation with  $5 \times 10^6$  NUGC4-T21 cells, mice were divided into six groups to receive various CAR-T cell treatments, as depicted in Figure 5(a). On day 30, the tumors were excised, paraffin-embedded, and prepared for immunohistochemical (IHC) analysis. (a) Representative images show immunohistochemical staining for human CD3+ T cells in tumor tissues on day 30, at 200× magnification. (b) Quantitative analysis of the percentages of CD3+ T cells is provided. (c) Multiplex immunohistochemistry images depict tumor tissues stained for CD3+ (green), CD8+ (yellow), Granzyme B+ (red), and nuclei counterstained with DAPI (blue) at 200× magnification. (d)-(e) Statistical analyses of CD8+ T cells (d) and CD3+ CD8+ Granzyme B+ T cells (e) are presented. (f) Long-term treatment protocol: NCG mice were subcutaneously inoculated with  $5 \times 10^6$  NUGC4-T21 cells. After 12 days, mice were treated with  $1 \times 10^6$  Mock T, 15 CAR-T or  $10 \times 15$  CAR-T cells ( $n = 5$  mice per group). (g)-(h) Survival times (g) and body weights (h) of the various treatment groups were evaluated. Results are expressed as mean  $\pm$  SD (b, d, e) and mean  $\pm$  SEM (h). Results were analyzed using one-way ANOVA (b, d, and e) and Log-rank test (g). \* $p < .05$ , \*\* $p < .01$ , \*\*\* $p < .001$ .

## Discussion

Although CAR-T-cell therapy for neoplasms shows promise, its effectiveness in solid tumors remains constrained primarily due to the inadequate infiltration of anti-tumor immune cells.<sup>31</sup> This limitation is exacerbated by a mismatch or absence of chemokine

migration signals at the tumor sites, hindering the aggregation of anti-tumor immune cells, especially cytotoxic T cells. Consequently, the scarcity of cytotoxic T cells contributes directly to a compromised anti-tumor immune response. To overcome this, we engineered CLDN18.2 CAR-T cells that overexpress

CXCL10 and IL15 (10 × 15 CAR). These 10 × 15 CAR-T cells enhanced the accumulation of CD8+ T cells at the tumor site and improved tumor control.

IL15 is essential in innate and adaptive immune cells.<sup>30</sup> The complex of IL15 and IL15R $\alpha$  activates cells expressing IL2R/IL15R $\beta\gamma$ ,<sup>32</sup> initiating downstream signaling pathways such as JAK1/JAK3 and STAT3/STAT5. These pathways promote T-cell proliferation,<sup>33</sup> inhibit IL2-induced apoptosis, and are crucial for CD8+ T cell proliferation.<sup>34</sup> Furthermore, CAR-T cells engineered with IL15 demonstrated superior anti-tumor efficacy and a higher stemness ratio compared to second-generation CAR-T cells.<sup>24</sup> Building on these findings, our study showed that the viability, proliferation, and division capabilities of 10 × 15 CAR were superior to those of 28z CAR. Similarly, like 15 CAR, 10 × 15 CAR-T cells secreting IL15 increased the proportion of CD8+ T cells and enhanced the stemness phenotype. Consequently, IL15-secreting CAR-T cells (15 CAR and 10 × 15 CAR) exhibited improved survival and immune responsiveness. Additionally, the 10 × 15 CAR-T cells showed enhanced CXCL10 secretion, further boosting their effectiveness.

The CXCL10-CXCR3 axis is a crucial chemokine signaling pathway for T cell migration.<sup>35</sup> CXCR3+ T cells are drawn toward higher concentrations by CXCL10 gradients, guiding their movement. Experiments with CXCL10 recombinant protein have shown that T cell migration is contingent upon the concentration of CXCL10. Previous research has verified that elevated CXCL10 concentrations in tumor regions promote immune cell aggregation, achieved either through direct injection<sup>36</sup> or via induction/mediation with fusion proteins or lysogenic adenovirus.<sup>18,37–40</sup> We demonstrated that CXCL10-engineered CAR-T cells (10 and 10 × 15 CAR-T cells) attracted more T cells than 28z CAR-T cells. Intriguingly, after seven days of co-culture with target cells, no marked difference was noted in T cell recruitment between the supernatants of the 10 CAR and 28z CAR groups. However, the recruitment by the 10 × 15 CAR group was notably more robust than that by the 10 CAR group, likely owing to the combined effects of IL15 and CXCL10. Considering that IL15 is vital for CAR-T cell proliferation and survival,<sup>41</sup> CXCL10 secretion by CAR-T cells is also enhanced by the presence of IL15. Thus, 10 × 15 CAR-T cells recruited significantly more T cells than 10 CAR cells under the influence of IL15, emphasizing the importance of integrating CXCL10 and IL15 in CAR-T cell designs.

The 10 × 15 CAR-T cells also exhibit beneficial effects in a xenograft tumor model using the gastric signet ring cell carcinoma cell line NUGC4-T21. Initially, conventional second-generation CAR-T cells showed potential for inhibiting tumor growth. Subsequently, IL15-secreting 15 CAR and 10 × 15 CAR cells exerted more substantial anti-tumor effects. Notably, the 10 × 15 CAR-T cells achieved more pronounced tumor regression compared to the 15 CAR-T cells. This enhanced efficacy might be attributed to the initial aggregation of T cells facilitated by the 10 × 15 CAR-T cells. Furthermore, the 10 × 15 CAR group exhibited a significantly higher accumulation of CD8+ T cells in tumor tissues compared to other groups. Consequently, the 10 × 15 CAR-T cells not only increased the intratumoral accumulation of CD8+ T cells but also enhanced

tumor suppression, highlighting the critical role of these engineered cells in therapeutic strategies for NUGC4-T21 xenograft tumor model.

Numerous research strategies have enhanced the responsiveness of solid tumors to T cells and CAR-T cells by modifying these cells with chemokines or their receptors. Modifications with CXCR1 or CXCR2 significantly boost the efficacy and targeted migration of CAR-T cells toward solid tumors, such as breast and pancreatic cancers.<sup>42</sup> Furthermore, CAR-T cells engineered with CXCL9 have shown increased anti-tumor efficacy and improved T cell infiltration in solid tumors.<sup>43</sup> However, after increasing chemokine concentrations within solid tumors, maintaining the persistence of CAR-T cells in the tumor environment emerges as a critical challenge. Interleukins, particularly IL2, IL7, and IL15, are essential for the proliferation and survival of CAR-T cells.<sup>44</sup> The co-expression of these interleukins with chemokine-modified CAR-T cells has made promising advancements. Specifically, 7 × 19 CAR-T cells have enhanced dendritic and T cell infiltration and CAR-T cell survival.<sup>26</sup> In zebrafish models, 15 × 19 CAR-T cells have increased T cell infiltration and cytotoxic activity against gastric cancer,<sup>29</sup> substantiating the adjunctive use of chemokines and interleukins in CAR-T cell therapy. We have demonstrated that 10 × 15 CAR-T cells enhance the infiltration of CD8+ T cells in a gastric xenograft tumor model and promote tumor control. Additionally, the ability of CXCL10 to recruit CXCR3+ T and NK cells, combined with IL15's role in boosting these cells' proliferation and survival, suggests that 10 × 15 CAR-T cells have considerable potential for treating solid tumors, especially in immune-excluded or desert tumor environments. Given that the murine models used in this study were immunodeficient, and the T cells originated from activated T cells, our observations on the proportion and functionality of inactive T cells and other immune cells within the TME are limited. We intend to select more representative animal models for further validation. Subsequently, we will explore the anti-tumor effects of 10 × 15 CAR-T cells in immunocompetent hosts and analyze the diversity and density of various immune cells within the TME.

In conclusion, we have enhanced human-derived anti-CLDN18.2 CAR-T cells using CXCL10 and IL15. The synergistic effects of these cytokines significantly improve the infiltration and accumulation of cytotoxic immune cells within tumors. Furthermore, 10 × 15 CAR-T cells facilitate the sustained proliferation and persistence of these cells at tumor sites, contributing to improved tumor control. Our research on 10 × 15 CAR-T cells has inspired further interest in advanced studies. For instance, integrating control switches could allow for precise targeting and controlled release of cytokines, thus increasing the specificity of anti-tumor activity. Therefore, 10 × 15 CAR-T cells represent a promising approach for immune cell therapy strategies in gastric tumors, offering significant clinical translational potential.

## Acknowledgments

We acknowledge Editage for English language editing support.

## Disclosure statement

No potential conflict of interest was reported by the author(s).

## Funding

This study was supported by the National Natural Science Foundation of China [No. 81972681].

## Author contributions

Conception and design: SN, SJ and ZZ.

Methodology: SN, YS, KH, FZ, LC and QM.

Analysis and interpretation of data: SN, YS, KH and WZ.

Writing the manuscript: SN.

Study supervision: SJ and ZZ.

All authors read and approved the final manuscript.

## Data availability statement

The data supporting the conclusions of this research are available from the corresponding authors upon reasonable request.

## References

- Sung H, Ferlay J, Siegel RL, Laversanne M, Soerjomataram I, Jemal A, Bray F. Global cancer statistics 2020: GLOBOCAN Estimates of incidence and mortality worldwide for 36 cancers in 185 Countries. *CA A Cancer J Clinicians*. 2021;71(3):209–249. doi:10.3322/caac.21660.
- Lei ZN, Teng QX, Tian Q, Chen W, Xie Y, Wu K, Zeng Q, Zeng L, Pan Y, Chen ZS. et al. Signaling pathways and therapeutic interventions in gastric cancer. *Signal Transduct Target Ther*. 2022;7(1):358. doi:10.1038/s41392-022-01190-w.
- Botta GP, Chao J, Ma H, Hahn M, Sierra G, Jia J, Hendrix AY, Nolte Fong JV, Ween A, Vu P, et al. Metastatic gastric cancer target lesion complete response with Claudin18.2-CAR T cells. *J Immunother Cancer*. 2024;12(2):12(2). doi:10.1136/jitc-2023-007927.
- Song Y, Tong C, Wang Y, Gao Y, Dai H, Guo Y, Zhao X, Wang Y, Wang Z, Han W, et al. Effective and persistent antitumor activity of HER2-directed CAR-T cells against gastric cancer cells in vitro and xenotransplanted tumors in vivo. *Protein Cell*. 2018;9(10):867–878. doi:10.1007/s13238-017-0384-8.
- Luo F, Qian J, Yang J, Deng Y, Zheng X, Liu J, Chu Y. Bifunctional  $\alpha$ HER2/CD3 RNA-engineered CART-like human T cells specifically eliminate HER2(+) gastric cancer. *Cell Res*. 2016;26(7):850–853. doi:10.1038/cr.2016.81.
- Jiang H, Shi Z, Wang P, Wang C, Yang L, Du G, Zhang H, Shi B, Jia J, Li Q, et al. Claudin18.2-specific chimeric antigen receptor engineered T cells for the treatment of gastric cancer. *J Natl Cancer Inst*. 2019;111(4):409–418. doi:10.1093/jnci/djy134.
- Lv J, Zhao R, Wu D, Zheng D, Wu Z, Shi J, Wei X, Wu Q, Long Y, Lin S, et al. Mesothelin is a target of chimeric antigen receptor T cells for treating gastric cancer. *J Hematol Oncol*. 2019;12(1):18. doi:10.1186/s13045-019-0704-y.
- Qi C, Gong J, Li J, Liu D, Qin Y, Ge S, Zhang M, Peng Z, Zhou J, Cao Y, et al. Claudin18.2-specific CAR T cells in gastrointestinal cancers: phase I trial interim results. *Nat Med*. 2022;28(6):1189–1198. doi:10.1038/s41591-022-01800-8.
- Zhang ZZ, Wang T, Wang XF, Zhang YQ, Song SX, Ma CQ. Improving the ability of CAR-T cells to hit solid tumors: Challenges and strategies. *Pharmacol. Research*. 2022;175:106036. doi:10.1016/j.phrs.2021.106036.
- Moon EK, Wang LS, Bekdache K, Lynn RC, Lo A, Thorne SH, Albelda SM. Intra-tumoral delivery of CXCL11 via a vaccinia virus, but not by modified T cells, enhances the efficacy of adoptive T cell therapy and vaccines. *Oncoimmunology*. 2018;7(3):e1395997. doi:10.1080/2162402X.2017.1395997.
- Fiori ME, Di Franco S, Villanova L, Bianca P, Stassi G, De Maria R. Cancer-associated fibroblasts as abettors of tumor progression at the crossroads of EMT and therapy resistance. *Mol Cancer*. 2019;18(1):70. doi:10.1186/s12943-019-0994-2.
- Foeng J, Comerford I, McColl SR. Harnessing the chemokine system to home CAR-T cells into solid tumors. *Cell Reports Medicine*. 2022;3(3):100543. doi:10.1016/j.xcrm.2022.100543.
- Newick K, O'Brien S, Moon E, Albelda SM. CAR T cell therapy for solid tumors. *Annu Rev Med*. 2017;68:139–152. doi:10.1146/annurev-med-062315-120245.
- Franciszkiwicz K, Boissonnas A, Boutet M, Combadière C, Mami-Chouaib F. Role of chemokines and chemokine receptors in shaping the effector phase of the antitumor immune response. *Cancer Res*. 2012;72(24):6325–6332. doi:10.1158/0008-5472.CAN-12-2027.
- Susek KH, Karvouni M, Alici E, Lundqvist A. The role of CXC chemokine receptors 1-4 on immune cells in the tumor microenvironment. *Front Immunol*. 2018;9:2159. doi:10.3389/fimmu.2018.02159.
- Ozga AJ, Chow MT, Luster AD. Chemokines and the immune response to cancer. *Immunity*. 2021;54(5):859–874. doi:10.1016/j.immuni.2021.01.012.
- Limagne E, Nuttin L, Thibaudin M, Jacquin E, Aucagne R, Bon M, Revy S, Barnestein R, Ballot E, Truntzer C. et al. MEK inhibition overcomes chemoimmunotherapy resistance by inducing CXCL10 in cancer cells. *Cancer Cell*. 2022;40(2):136–152.e12. doi:10.1016/j.ccell.2021.12.009.
- Jie X, Chen Y, Zhao Y, Yang X, Xu Y, Wang J, Meng R, Zhang S, Dong X, Zhang T, et al. Targeting KDM4C enhances CD8+T cell mediated antitumor immunity by activating chemokine CXCL10 transcription in lung cancer. *J Immunother Cancer*. 2022;10(2):e003716. doi:10.1136/jitc-2021-003716.
- Xu K, Yin X, Zhou B, Zheng X, Wang H, Chen J, Cai X, Gao H, Xu X, Wang L, et al. FOSL2 promotes intertumoral infiltration of T cells and increases pathological complete response rates in locally advanced rectal cancer patients. *Cancer Lett*. 2023;562:216145. doi:10.1016/j.canlet.2023.216145.
- Yan Y, Zheng L, Du Q, Yazdani H, Dong K, Guo Y, Geller DA. Interferon regulatory factor 1(IRF-1) activates anti-tumor immunity via CXCL10/CXCR3 axis in hepatocellular carcinoma (HCC). *Cancer Lett*. 2021;506:95–106. doi:10.1016/j.canlet.2021.03.002.
- Wang X, Lu XL, Zhao HY, Zhang FC, Jiang XB. A novel recombinant protein of IP10-EGFRvIIIscFv and CD8(+) cytotoxic T lymphocytes synergistically inhibits the growth of implanted glioma in mice. *Cancer Immunol Immunother*. 2013;62(7):1261–1272. doi:10.1007/s00262-013-1426-6.
- Xia L, Tian E, Yu M, Liu C, Shen L, Huang Y, Wu Z, Tian J, Yu K, Wang Y, et al. RORyt agonist enhances anti-PD-1 therapy by promoting monocyte-derived dendritic cells through CXCL10 in cancers. *J Exp Clin Cancer Res*. 2022;41(1):155. doi:10.1186/s13046-022-02289-2.
- Alizadeh D, Wong RA, Yang X, Wang D, Pecoraro JR, Kuo CF, Aguilar B, Qi Y, Ann DK, Starr R, et al. IL15 enhances CAR-T cell antitumor activity by reducing mTORC1 activity and preserving their stem cell memory phenotype. *Cancer Immunol Res*. 2019;7(5):759–772. doi:10.1158/2326-6066.CIR-18-0466.
- Lanitis E, Rota G, Kostis P, Ronet C, Spill A, Seijo B, Romero P, Dangaj D, Coukos G, Irving M. Optimized gene engineering of murine CAR-T cells reveals the beneficial effects of IL-15 coexpression. *J Exp Med*. 2021;218(2). doi:10.1084/jem.20192203.
- Gargett T, Ebert LM, Truong NTH, Kollis PM, Sedivakova K, Yu W, Yeo ECF, Wittwer NL, Gliddon BL, Tea MN. et al. GD2-targeting CAR-T cells enhanced by transgenic IL-15 expression are an effective and clinically feasible therapy for glioblastoma. *J Immunother Cancer*. 2022;10(9):e005187. doi:10.1136/jitc-2022-005187.
- Adachi K, Kano Y, Nagai T, Okuyama N, Sakoda Y, Tamada K. IL-7 and CCL19 expression in CAR-T cells improves immune cell infiltration and CAR-T cell survival in the tumor. *Nat Biotechnol*. 2018;36(4):346–351. doi:10.1038/nbt.4086.

27. Pang N, Shi J, Qin L, Chen A, Tang Y, Yang H, Huang Y, Wu Q, Li X, He B, et al. IL-7 and CCL19-secreting CAR-T cell therapy for tumors with positive glypican-3 or mesothelin. *J Hematol Oncol.* 2021;14(1):118. doi:10.1186/s13045-021-01128-9.
28. Luo H, Su J, Sun R, Sun Y, Wang Y, Dong Y, Shi B, Jiang H, Li Z. Coexpression of IL7 and CCL21 increases efficacy of CAR-T cells in solid tumors without requiring preconditioned lymphodepletion. *Clin Cancer Res.* 2020;26(20):5494–5505. doi:10.1158/1078-0432.CCR-20-0777.
29. Zhou Z, Li J, Hong J, Chen S, Chen M, Wang L, Lin W, Ye Y. Interleukin-15 and chemokine ligand 19 enhance cytotoxic effects of chimeric antigen receptor T cells using zebrafish xenograft model of gastric cancer. *Front Immunol.* 2022;13:1002361. doi:10.3389/fimmu.2022.1002361.
30. Pilipow K, Roberto A, Roederer M, Waldmann TA, Mavilio D, Lugli E. IL15 and T-cell stemness in T-cell-based cancer immunotherapy. *Cancer Res.* 2015;75(24):5187–5193. doi:10.1158/0008-5472.CAN-15-1498.
31. Sterner RC, Sterner RM. CAR-T cell therapy: current limitations and potential strategies. *Blood Cancer J.* 2021;11(4):69. doi:10.1038/s41408-021-00459-7.
32. Van den Bergh JM, Lion E, Van Tendeloo VF, Smits EL. IL-15 receptor alpha as the magic wand to boost the success of IL-15 antitumor therapies: The upswing of IL-15 transpresentation. *Pharmacol. Therapeut.* 2017;170:73–79. doi:10.1016/j.pharmthera.2016.10.012.
33. Waldmann TA, Miljkovic MD, Conlon KC. Interleukin-15 (dys) regulation of lymphoid homeostasis: Implications for therapy of autoimmunity and cancer. *J. Experiment. Med.* 2020;217(1). doi:10.1084/jem.20191062.
34. Hangasky JA, Chen W, Dubois SP, Daenthanasanmak A, Müller JR, Reid R, Waldmann TA, Santi DV. A very long-acting IL-15: implications for the immunotherapy of cancer. *J Immunother Cancer.* 2022;10(1):e004104. doi:10.1136/jitc-2021-004104.
35. Zlotnik A, Yoshie O. Chemokines: a new classification system and their role in immunity. *Immunity.* 2000;12(2):121–127. doi:10.1016/S1074-7613(00)80165-X.
36. Arenberg DA, White ES, Burdick MD, Strom SR, Strieter RM. Improved survival in tumor-bearing SCID mice treated with interferon-gamma-inducible protein 10 (IP-10/CXCL10). *Cancer Immunol Immunother.* 2001;50(10):533–538. doi:10.1007/s00262-001-0231-9.
37. Li X, Lu M, Yuan M, Ye J, Zhang W, Xu L, Wu X, Hui B, Yang Y, Wei B, et al. CXCL10-armed oncolytic adenovirus promotes tumor-infiltrating T-cell chemotaxis to enhance anti-PD-1 therapy. *Oncoimmunology.* 2022;11(1):2118210. doi:10.1080/2162402X.2022.2118210.
38. Wennerberg E, Kremer V, Childs R, Lundqvist A. CXCL10-induced migration of adoptively transferred human natural killer cells toward solid tumors causes regression of tumor growth in vivo. *Cancer Immunol Immunother.* 2015;64(2):225–235. doi:10.1007/s00262-014-1629-5.
39. Barreira da Silva R, Laird ME, Yatim N, Fiette L, Ingersoll MA, Albert ML. Dipeptidylpeptidase 4 inhibition enhances lymphocyte trafficking, improving both naturally occurring tumor immunity and immunotherapy. *Nat Immunol.* 2015;16(8):850–858. doi:10.1038/ni.3201.
40. Barash U, Zohar Y, Wildbaum G, Beider K, Nagler A, Karin N, Ilan N, Vlodaysky I. Heparanase enhances myeloma progression via CXCL10 downregulation. *Leukemia.* 2014;28(11):2178–2187. doi:10.1038/leu.2014.121.
41. Battram AM, Bachiller M, Lopez V, Fernández de Larrea C, Urbano-Ispizua A, Martín-Antonio B. IL-15 enhances the persistence and function of BCMA-Targeting CAR-T cells compared to IL-2 or IL-15/IL-7 by limiting CAR-T cell dysfunction and differentiation. *Cancers Basel.* 2021;13(14):3534. doi:10.3390/cancers13143534.
42. Jin L, Tao H, Karachi A, Long Y, Hou AY, Na M, Dyson KA, Grippin AJ, Deleyrolle LP, Zhang W, et al. CXCR1- or CXCR2-modified CAR T cells co-opt IL-8 for maximal antitumor efficacy in solid tumors. *Nat Commun.* 2019;10(1):4016. doi:10.1038/s41467-019-11869-4.
43. Tian Y, Wen C, Zhang Z, Liu Y, Li F, Zhao Q, Yao C, Ni K, Yang S, Zhang Y. CXCL9-modified CAR T cells improve immune cell infiltration and antitumor efficacy. *Cancer Immunol Immunother.* 2022;71(11):2663–2675. doi:10.1007/s00262-022-03193-6.
44. Luo M, Gong W, Zhang Y, Li H, Ma D, Wu K, Gao Q, Fang Y. New insights into the stemness of adoptively transferred T cells by  $\gamma$ c family cytokines. *Cell Commun Signal.* 2023;21(1):347. doi:10.1186/s12964-023-01354-3.